Sensors & Diagnostics

PAPER

View Article Online
View Journal | View Issue

Cite this: *Sens. Diagn.*, 2024, **3**, 1976

A self-assembling protein–DNA complex with an inbuilt DNA release system for quantitative immuno-PCR applications†

A. E. Sorenson and P. M. Schaeffer *

Site-specific protein : DNA conjugation is gaining increasing importance in detection technologies such as quantitative immuno-PCR (qIPCR). Until now, DNA-binding proteins have been a relatively untapped source of protein : DNA conjugation systems. In *Escherichia coli*, the biotin protein ligase (BirA) is a biotin-dependent DNA-binding protein that offers a means to connect a protein of interest (POI) with DNA. Here, we explored BirA as a unique on–off protein : DNA connection switch for the production of self-assembling POI : DNA conjugates. Green fluorescent protein (GFP) is a versatile protein tag and reporter, commonly quantified by fluorescence detection. However, low GFP concentrations are challenging to detect and require more sensitive methods. A multitude of high-affinity antibodies are available for capture and detection of GFP as an affinity tag. As such, a well-characterised GFP-tagged BirA (BirA-GFP) was selected for the development and validation of an innovative qIPCR platform technology. The unique principle of this assay involves the assembly of two BirA-GFP with the *bioO* repressor DNA sequence in the presence of ATP and biotin. The resulting high affinity *bioO* : BirA-GFP complex can be applied in various formats to detect the presence of anti-GFP IgG as well as GFP immobilised on a surface. Complete release of the quantifiable *bioO* DNA can easily be achieved by omitting ATP and biotin in the final elution step. The new BirA-based qIPCR assay enabled picomolar ($\geq 10^{-12}$ M) detection of GFP and anti-GFP IgG as well as their affinity profiling.

Received 27th June 2024,
Accepted 14th October 2024

DOI: 10.1039/d4sd00225c

rsc.li/sensors

Introduction

Site-selective conjugation of protein with DNA is gaining importance in protein detection and display technologies.[1,2] Immuno-PCR assays are reliant on covalent or non-covalent protein : DNA conjugation to significantly increase the sensitivity of immunoassays by several orders of magnitude.[3] High-affinity DNA-binding proteins are a relatively untapped source of connecting systems, with Tus being the only example of an *Escherichia coli* protein that has been successfully translated into a versatile protein : DNA connection system for the production of qIPCR detection devices.[3–8]

In *E. coli*, biotin protein ligase (BirA) is a biotin-dependent DNA binding protein. The primary function of BirA is to covalently attach biotin to the biotin carboxyl carrier protein (BCCP) subunit of acetyl-coA carboxylase (ACC).[9–11] The biotin prosthetic group is essential for malonyl-CoA synthesis. The process involves sequential binding of biotin followed by ATP to BirA to yield the adenylated intermediate biotinyl-5′-AMP (bio-5′-AMP) with concomitant release of pyrophosphate.[12] Once formed, bio-5′-AMP dissociates 1000-fold slower (half-life >30 min) from *E. coli* BirA than biotin.[13,14] The bio-5′-AMP bound BirA is the holoenzyme (holoBirA) that catalyses the formation of an amide bond between biotin and a specific lysine residue of the BCCP subunit within the ACC complex. BirA has been successfully developed for site-specific biotinylation of proteins containing small peptide tags such as the AviTag both *in vivo* and *in vitro*.[15–17] The commercial AviTag system is now routinely applied for protein biotinylation.[18] However, despite the high profile of *E. coli* BirA in protein biotinylation, its well-characterised DNA binding property[19] has not yet been exploited.

E. coli holoBirA regulates expression of *bio* genes and subsequently biotin synthesis through its tight binding to the biotin operator (*bioO*), a 40 bp inverted DNA repeat that overlaps and controls both biotin operon promoters.[20–28] Binding of *E. coli* holoBirA to *bioO* yields a 2 : 1 protein : DNA complex with nanomolar affinity.[29] The affinity of *E. coli* BirA for *bioO* increases substantially when bound to biotin and even further when it is bound to bio-5′-AMP in the presence

Molecular and Cell Biology, College of Public Health, Medical and Veterinary Sciences, James Cook University, The Science Place, Building 142, University Drive, Douglas, QLD 4811, Australia. E-mail: patrick.schaeffer@jcu.edu.au; Tel: +61 (0)7 4781 4448

† Electronic supplementary information (ESI) available. See DOI: https://doi.org/10.1039/d4sd00225c

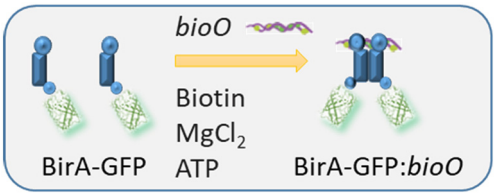

Fig. 1 Principle of *E. coli* BirA : *bioO* self-assembly. Two *E. coli* BirA-GFP bind to biotin and ATP and assemble with *bioO* into a stable protein : DNA complex following formation of bio-5′-AMP.

of Mg^{2+} ions.[30] The dissociation half-life for *E. coli* holoBirA : *bioO* is 400 s in a buffer containing 200 mM KCl.[21] *E. coli* BirA requires Mg^{2+} ions to catalyse the formation of bio-5'AMP. It is proposed that it is the formation of bio-5′-AMP that triggers the dimerization of *E. coli* holoBirA and increases its affinity for *bioO*.[25] As such, *E. coli* BirA offers the possibility of dimerizing two proteins of interest such as GFP through a tightly-controlled association mechanism with *bioO* (Fig. 1).

GFP-tagged proteins are useful reporter molecules that can be detected with flow cytometry or imaging applications to monitor physiological processes, detect transgenic expression *in vivo*, and visualize protein localization.[31] The autofluorescence of GFP can easily be measured at nanomolar and higher concentrations using a fluorescence plate reader. However, ultrasensitive quantification of GFP-tagged proteins is still challenging. Low expression or fluorescence can be amplified with anti-GFP antibodies and antibody conjugates, and detected using imaging, western blotting, flow cytometry and immunoassays. Quantification of picomolar concentrations of GFP-tagged proteins, expressed, secreted or circulating in complex matrices is not trivial. A TT-lock qIPCR assay has been shown to detect pM concentrations of GFP and GFP-fusion proteins.[4,6,7] GFP-tagged nanobodies[32] and combinations of bispecific antibodies with affinity towards GFP or comprising a GFP[33–37] present new application areas for ultrasensitive GFP detection.

We have previously shown that GFP-tagged *E. coli* BirA (*E. coli* BirA-GFP) is fully functional, including its binding to *bioO*.[18,38] Here, we evaluated *E. coli* BirA as a unique on–off protein : DNA connection switch for the production and release of self-assembling protein : DNA conjugates. We present the first application of this system with *E. coli* BirA-GFP as a useful qIPCR detection device for GFP quantitation and anti-GFP antibody affinity profiling.

Materials and methods

Protein targets

E. coli BirA-GFP, *B. pseudomallei* BirA-GFP and *M. tuberculosis* BirA-GFP were expressed and purified as previously described.[19,39,40] BirA-GFP were resuspended in BirA buffer (25 mM Tris pH 8, 100 mM NaCl, 5% v/v glycerol). Protein concentrations were determined by Bradford assay and protein purity by SDS-PAGE.

Differential scanning fluorimetry of GFP-tagged proteins (DSF-GTP)

E. coli BirA-GFP (1 μM) in PBS-T (ProteOn running buffer: phosphate buffered saline, pH 7.4, 0.005% Tween 20) in the presence of various combinations of ligands ($MgCl_2$, biotin, ATP and *bioO*) was incubated at room temperature (RT) for 5 min then heated in a real-time thermocycler (CFX96, Bio-Rad) from 25–90 °C, increasing in 0.5 °C increments every 30 s. Final ligand concentrations were 5 mM, 1 mM, 1 mM and 1 μM respectively for $MgCl_2$, biotin, ATP and *bioO*. A series of experiments was also performed in PBS-T with 300 mM final NaCl (PBS-T (HS)). Data were analysed using Bio-Rad CFX Maestro software for transition midpoint (T_m) determination as previously described.[41,42]

qPCR standard curve and data analyses

Solutions of 1 μM *bioO* specific primers (in water) were spiked with *bioO* template to yield final concentrations ranging from 250 pM to 50 fM. qPCR reactions contained 10 μL of the above spiked *bioO* solutions and 10 μL Sso Advanced SYBR Green qPCR master mix (Bio-Rad). The qPCR protocol was performed in a Bio-Rad CFX96 thermocycler with an initial incubation of 10 min at 95 °C followed by 40 cycles of 95 °C for 10 s and 60 °C for 20 s. All reactions were run in duplicate. Fluorescence threshold, window-of-linearity and PCR efficiency were determined using LinRegPCR software (Heart Failure Research Center).[43] Linear regression was also performed using GraphPad Prism 7.04.

E. coli BirA : bioO qIPCR for development and evaluation phase

Polyclonal goat anti-GFP IgG (Abcam ab6673) was adsorbed (*i.e.* dilutions ranging from 16.5 nM to 100 fM in PBS-T (ProteOn, Bio-Rad)) onto the surface of Nunc clear polystyrene (PS) U96 MicroWell™ plate with a MaxiSorp™ surface for solid phase immunoassays (Nunc, 449824) overnight at RT in 50 μL aliquots. Microplates were blocked for 1 h at RT with 100 μL 1% BSA in PBS-T. *E. coli* BirA-GFP : *bioO* was assembled at 1 μM at RT for 15 min in PBS-T with 1 mM biotin and 1 mM ATP (PBS-TBA). The *E. coli* BirA-GFP : *bioO* complex was diluted to 2.5 nM and in PBS-TBA and 50 μL applied to the well for 30 min at RT. The diluted complex was aspirated and the microplates were washed four times with PBS-TBA (300 μL). The *bioO* was released from the complex with the addition of 50 μL of 1 μM *bioO*-specific primers for 30 min at RT (see ESI† for sequence details of the *bioO* template sequence and primers). Supernatant (10 μL) was combined with 10 μL Sso Advanced SYBR Green qPCR master mix (Bio-Rad) in 96-well hard-shell full-skirted PCR plates (Bio-Rad). Negative controls were performed as before without antibody in PBS-T and measured the background signal (indirect and direct non-specific *bioO* binding to well surface). All qPCRs were run as above in duplicate. Additional experiments were conducted as described with assembly,

dilution and wash steps performed in PBS-TBA with 5 mM $MgCl_2$ (see ESI†).

E. coli BirA : bioO qIPCR dissociation rates

Polyclonal goat anti-GFP IgG (Abcam ab6673) was adsorbed at 10 nM in PBS (ProteOn, Bio-Rad) onto the surface of Nunc clear polystyrene (PS) U96 MicroWell™ plate with a MaxiSorp™ surface for solid phase immunoassays (Nunc, 449824) overnight at RT in 100 μL aliquots. Microplates were blocked for 1 h at RT with 200 μL 1% BSA in PBS-T with shaking at 200 RPM. *E. coli* BirA-GFP : *bioO* was assembled as described in PBS-TBA and in parallel with PBS-TBA with 5 mM $MgCl_2$ (PBS-TBA + $MgCl_2$). Complexes were diluted to 2.5 nM and in PBS-TBA or PBS-TBA + $MgCl_2$ and 150 μL applied to the well for 30 min at RT with shaking at 200 RPM. Aspiration and wash steps were performed as described previously with PBS-TBA or PBS-TBA + $MgCl_2$. The *bioO* was released from the complex with the addition of 150 μL of 1 μM *bioO*-specific primers for 45 min at RT, with 10 μL aliquots of supernatant taken at 0, 2, 4, 8, 13, 30 and 45 min. qPCR were performed in duplicate as described previously.

E. coli BirA : bioO bridging qIPCR

GFP was adsorbed (dilutions ranging from 1 μM to 1 pM in PBS-T (ProteOn, Bio-Rad)) onto the surface of Nunc clear polystyrene (PS) U96 MicroWell™ MaxiSorp™ plate (Nunc, 449824) in 50 μL aliquots for 2 h at RT with shaking at 200 RPM. Microplates were blocked for 30 min at RT with 100 μL 1% BSA in PBS-T with shaking. *E. coli* BirA-GFP : *bioO* was assembled and diluted to 2.5 nM in PBS-TBA. Polyclonal goat anti-GFP IgG (Abcam ab6673) and HRP-conjugated protein G were added at 1 μg mL^{-1} to the diluted complex and 50 μL of the mixture applied to the wells for 30 min at RT with shaking. Aspiration and wash steps were performed as described previously. The *bioO* was released from the complex with the addition of 50 μL of 1 μM *bioO*-specific primers for 30 min at RT. qPCR were performed using 10 μL aliquots as described previously. TMB solution (20 μL, Sigma-Aldrich) was added to the remaining 40 μL in the wells. The reaction was developed for 15 min at RT, stopped with H_2SO_4 (5 μL 2 M) and read at 450 nm. The dilution of the TMB reagent yields a corresponding reduction in signal strength.

E. coli BirA : bioO qIPCR for antibody profiling

Polyclonal chicken anti-GFP (Aves, AB_2307313), polyclonal biotinylated goat anti-GFP (Abcam, ab6658) and monoclonal mouse anti-6x His (Abcam, ab18184) were adsorbed onto the surface of Nunc clear polystyrene (PS) U96 MicroWell™ MaxiSorp™ plate (Nunc, 449824) at 2 μg mL^{-1} in 50 mM phosphate buffer, pH 7.8 in 50 μL aliquots overnight at 4 °C. Microplates were washed and blocked as described previously. *E. coli* BirA-GFP : *bioO* was assembled and serially diluted (2.5 nM to 0.156 nM) and applied in 50 μL aliquots for 1 h at RT. Aspiration, wash, and dissociation steps were performed as described previously. qPCR was performed with BioRad iTaq Universal SYBR green supermix with an initial incubation of 2 min at 95 °C followed by 40 cycles of 95 °C for 10 s and 60 °C for 20 s. qPCR were performed in duplicate.

Results and discussion

Stability of *E. coli* BirA-GFP : bioO in the presence and absence of $MgCl_2$

The pH and salt effects on *E. coli* BirA activity, dimerization and *bioO* binding have previously been examined.[44–46] We were particularly interested in the stability of the *E. coli* BirA-GFP : *bioO* complex, bound to both biotin and ATP in the absence of Mg^{2+} ions, which has never been investigated. We hypothesized that in the absence of Mg^{2+} ions, the binding of ATP and biotin to *E. coli* BirA would increase its affinity for *bioO* compared to the biotin-bound form without freezing the complex through formation of bio-5′-AMP. Here, the DSF-GTP technology[41,42,47] that had previously been validated for *E. coli*, *Burkholderia pseudomallei* and *Mycobacterium tuberculosis* BirA-GFP[19,39,40,48] provided us with an ideal assay to examine the effect of Mg^{2+} ions on the *E. coli* BirA-GFP and its various complexes in different buffer conditions.

First, we compared the effect of biotin (1 mM), ATP (1 mM) and $MgCl_2$ (5 mM), and combinations thereof on the transition midpoint (T_m) values of *E. coli* BirA-GFP (1 μM) in PBS-T, then in PBS-T high salt (HS) (Fig. 2, S1A and B†). The increase in T_m value for *E. coli* BirA-GFP when both ATP and biotin are present reflects formation of significant stabilizing interactions upon binding of ATP to the biotin-bound species. $MgCl_2$ only increases the T_m of *E. coli* BirA-GFP when in presence of both biotin and ATP which is likely due to the formation of the holoenzyme and slow dissociation of bio-5′-AMP.

Next, we compared the binding of *E. coli* BirA-GFP to *bioO* (Fig. 2 and S1C–F†) with combinations of biotin, ATP, $MgCl_2$ as well as *bioO* (1 μM) in PBS-T and PBS-T (HS). The presence of *bioO* significantly increased the T_m of all tested forms of *E. coli* BirA, *i.e.* biotin-bound, biotin/ATP-bound and holoBirA, suggesting the formation of discrete protein : DNA complexes for these species in PBS-T. Previous EMSA and DNA footprinting data support these findings.[19,30] Stark differences in T_m between these *E. coli* BirA-GFP : *bioO* complexes are evident. The data for *E. coli* BirA and *bioO* is consistent with a low affinity protein : DNA complex. The difference in T_m between biotin-bound *E. coli* BirA-GFP and biotin-bound *E. coli* BirA-GFP : *bioO* indicates a significant increase in *bioO* binding affinity.

The T_m values for both biotin/ATP-bound *E. coli* BirA-GFP : *bioO* and holoBirA-GFP : *bioO* could not be determined in PBS-T due to the extreme thermal stabilization effects of *bioO*. Here, the PBS-T (HS) conditions were essential to weaken the DNA binding affinity of *E. coli* BirA-GFP sufficiently to measure and compare the T_m values of all *bioO* complexes (Fig. 2). The data clearly show that the stability of the biotin/ATP-bound *E. coli* BirA-GFP for *bioO* is

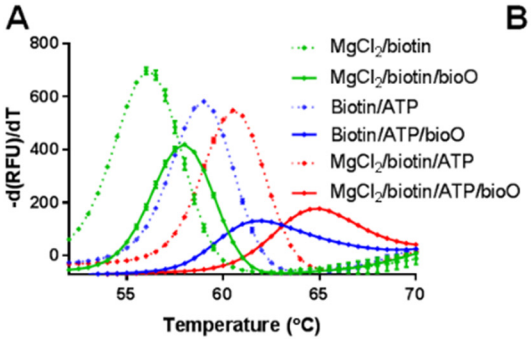

B

	Ec BirA-GFP T_m (°C)			
	PBS		PBS (HS)	
Ligand	(-)	*bioO*	(-)	*bioO*
None	45.0	-	47	-
$MgCl_2$	45.0	47.5	46.7	47.2
Biotin	55.0	-	-	-
$MgCl_2$/biotin	55.0	60.5	56	58
Biotin/ATP	58.7	*	59	62
$MgCl_2$/biotin/ATP	60.5	*	60.5	65

Fig. 2 Ligand effects on *E. coli* BirA-GFP melt-curves in PBS-T and PBS-T (HS). A) *E. coli* BirA-GFP (1 μM) was incubated for 10 min at RT with combinations of biotin (1 mM), ATP (1 mM) and $MgCl_2$ (5 mM) in PBS-T (HS) prior to analysis by DSF-GTP melt-curve protocol (35–90 °C at 0.5 °C/30 s). B) *E. coli* (Ec) BirA-GFP T_m with combinations of biotin, ATP, $MgCl_2$ and *bioO* (1 μM). T_m were analyzed (see Fig. S1† for full data). Data represent averages and SD of three melt-curves. (–): not tested. (*): could not be determined.

intermediate between the biotin-bound and holoenzyme species, providing support to our working hypothesis.

Development and evaluation of the *E. coli* BirA : bioO qIPCR

Further to our encouraging DSF-GTP data, we hypothesized that the biotin/ATP-bound *E. coli* BirA-GFP : *bioO* complex formed in the absence of Mg^{2+} ions, despite being highly stable, could have the advantage of dissociating rapidly upon removal of ATP and biotin, offering a useful DNA release trigger mechanism for qIPCR detection and other display applications. In this scenario, ATP and biotin can simply be omitted in the final qIPCR elution step to promote rapid *bioO* DNA template dissociation.

In our proof-of-concept qIPCR setup (Fig. 3A), anti-GFP IgG in solutions ranging from 10^{-13} to 10^{-8} M were physisorbed

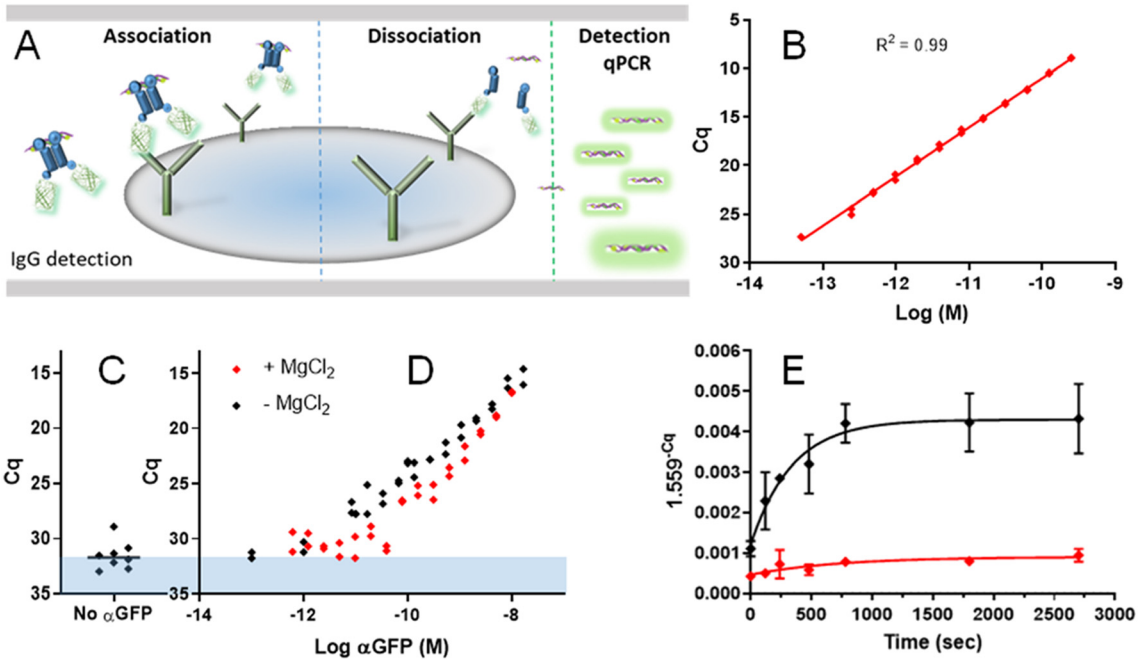

Fig. 3 qIPCR detection of preadsorbed polyclonal anti-GFP IgG with *E. coli* BirA-GFP : *bioO*. A) Schematic representation of the qIPCR platform principle involving binding of the *E. coli* BirA-GFP : *bioO* to preadsorbed anti-GFP IgG (association) followed by release of *bioO* (dissociation) and qPCR detection. B) qPCR standard curve for *bioO* (slope = −5.064). All replicates are shown. See ESI† for sequence details of the *bioO* template sequence and primers. C) Background control qIPCR were performed by omitting IgG with biotin/ATP-bound *E. coli* BirA-GFP : *bioO* in PBS-T (PBS-TBA – $MgCl_2$, black diamonds). All replicates are shown. D) Comparison of qIPCR detection of preadsorbed polyclonal anti-GFP IgG with biotin/ATP-bound *E. coli* BirA-GFP : *bioO* (PBS-TBA – $MgCl_2$, black diamonds and *E. coli* holoBirA-GFP : *bioO* (PBS-TBA + $MgCl_2$, red diamonds). Concentrations of IgG (αGFP) are as indicated. All replicates are shown. The slope is steeper in the holoenzyme conditions (PBS-TBA + $MgCl_2$) resulting in a loss of detection performance. It is important to note that buffer compositions are different and data are thus not directly comparable as background values are differently affected. All replicates are shown. E) qIPCR *bioO* dissociation time-course experiment for complexes formed in the presence or absence of $MgCl_2$ was set at the highest concentration of αGFP IgG. Averages of two datapoints and standard deviations are shown. The dissociation half-life for *bioO* in the absence of $MgCl_2$ (black diamonds) is 234.7 s calculated with a PCR efficiency of 1.559 (LinRegPCR).

onto the wells of a 96-well plate. After the blocking and wash steps, 50 μL of *E. coli* BirA-GFP : *bioO* (2.5 nM in PBS-TBA) were added for 30 min at RT. Following four wash steps with PBS-TBA, *bioO* was released from the complex in a 50 μL aqueous primer mix solution (*i.e.* no ATP nor biotin) for 30 min, of which 10 μL were used for qPCR analysis.

A qPCR standard curve spanning over a 4 log dynamic range with a R^2 correlation coefficient of 0.998 was obtained with our selected *bioO* qPCR DNA template and primers (Fig. 3B). A series of background control qIPCR were set up without IgG (Fig. 3C), as well as by replacing *E. coli* BirA-GFP with either *B. pseudomallei* or *M. tuberculosis* BirA-GFP which do not bind *bioO* (Fig. S2B–D†). At a BirA-GFP : *bioO* detection device concentration of 2.5 nM, Cq values ~32 were obtained for the background control reactions which is equivalent to ~10^{-14} M *bioO* (Cq value ~32) as derived from the standard curve (*cf.* Fig. 3B and C). The qIPCR background Cq values are due to the concentration-dependent non-specific adsorption and dissociation of the *bioO* DNA (directly and indirectly) to and from a well's surface. Thus, background qIPCR Cq values represent the absolute limit of detection of the qIPCR which are mirrored by the *M. tuberculosis* and *B. pseudomallei* BirA-GFP data (Fig. S2†).

Our proof-of-concept qIPCR assay could detect *bioO* molecules dissociating from wells that were coated with a ≥10^{-12} M anti-GFP IgG suspension (Fig. 3D). The binding affinity and kinetics of the *E. coli* BirA-GFP : *bioO* detection device are unknown in the PBS-TBA conditions and cannot be examined using traditional methods such as SPR due to the changes in binding and elution conditions as well as differences in surfaces. Hence, we performed the same qIPCR assay in the presence of $MgCl_2$ to evaluate the *E. coli* holoBirA-GFP : *bioO* complex as a detection device. In these conditions, the qIPCR was less sensitive with a detection limit for anti-GFP IgG >10^{-11} M (Fig. 3D *cf.* red diamonds). To shed further light onto these findings, we performed a time-course experiment with complexes formed in the presence or absence of $MgCl_2$ aiming at comparing the dissociation kinetics of *bioO* from *E. coli* BirA-GFP after the qIPCR wash steps (Fig. 3E). The data clearly show that when the device is prepared without $MgCl_2$, significantly more *bioO* molecules bind to the wells and they also dissociate faster after the wash steps. As such, the stability of the protein : DNA connection is not the only essential attribute of our ultrasensitive qIPCR detection device. Here, increased binding and fast release of *bioO* DNA are both desirable to improve the analytical detection performance of our *E. coli* BirA : *bioO* qIPCR assay. Alternative DNA release mechanisms triggered by either BCCP or the AviTag peptide in conjunction with high affinity mutants[49] like $BirA^{G154D}$ could be envisaged in qIPCR applications, albeit with obvious drawbacks, *e.g.* increased complexity and cost.

Bridging immunoassay format

Sensitive bridging immunoassays are useful for the detection of anti-drug antibodies[50,51] taking advantage of their dimeric structure, and qIPCR techniques have demonstrated superior sensitivity.[52,53] Here, we evaluated the *E. coli* BirA-GFP : *bioO* in a bridging qIPCR format (Fig. 4A). We compared the performance of the *E. coli* BirA-GFP : *bioO* with a commercial protein G-peroxidase conjugate in the same wells, in identical conditions (Fig. 4B, *cf.* blue diamonds). A plateau is reached with a 10^{-7} M GFP suspension for well coating with either detection method (Fig. 4B). However, the detection range is much narrower with the protein G-peroxidase. Overall, the analytical sensitivity and dynamic range of the *E. coli* BirA-GFP : *bioO* device is impressively high compared to the peroxidase conjugate (~10 000 fold more sensitive, *cf.* Fig. 4B).

Antibody and surface profiling

SPR is the gold standard method for antibody affinity and concentration determination. However, it cannot be applied to antibody samples containing other protein contaminants and does not mirror the surface interactions occurring in an ELISA format. Here we showcase an important application of the *E. coli* BirA-GFP : *bioO* detection device in antibody and capture surface profiling. The *bioO* release system is particularly useful in profiling surfaces coated with high affinity binders with

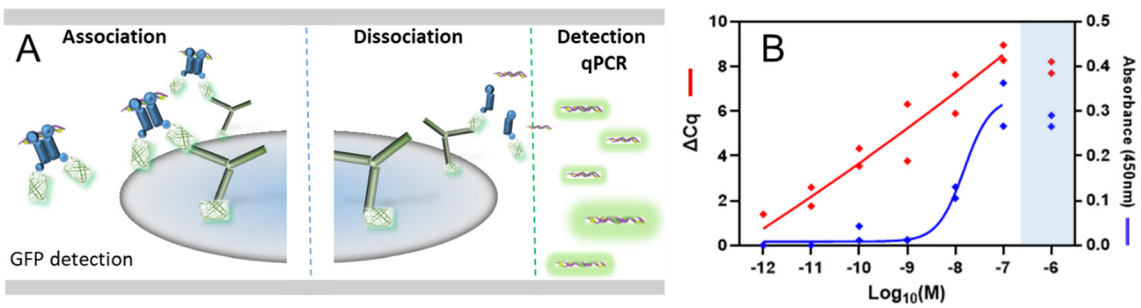

Fig. 4 Bridging qIPCR format for the detection of GFP. A) Schematic representation of the bridging qIPCR principle involving binding of anti-GFP IgG to preadsorbed GFP. After the wash step, *E. coli* BirA-GFP : *bioO* is added and bound to anti-GFP IgG (association). The *bioO* is then released following the wash steps (dissociation) and detected by qPCR. B) Detection of preadsorbed GFP with *E. coli* BirA-GFP : *bioO* qIPCR (Cq values, red diamonds) and protein G-peroxidase (absorbance (Abs.) reading at 450 nm, blue diamonds). The same reaction wells were used for both G-peroxidase and qIPCR detection strategies to allow direct comparison of datasets. GFP concentrations are as indicated. All replicates are shown. Data were fit excluding the highest concentration due to a hook effect shaded in grey.

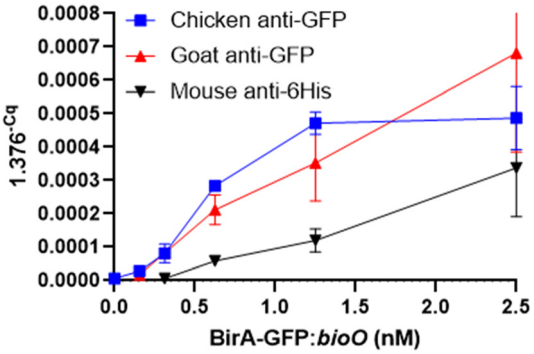

Fig. 5 Antibody surface profiling with *E. coli* BirA-GFP : *bioO*. Detection of physisorbed polyclonal chicken anti-GFP, biotinylated polyclonal goat anti-GFP and mouse monoclonal anti-6His with biotin/ATP-bound *E. coli* BirA-GFP : *bioO* at 0.156, 0.313, 0.625, 1.250 and 2.500 nM. The BioRad iTaq Universal SYBR green supermix has a PCR efficiency of 1.376 (LinRegPCR) with the *bioO* primer set. All antibodies were physisorbed at 2 μg mL^{-1}. Background control qIPCR were performed by omitting antibodies. Averages of two datapoints and standard deviations are shown. Upper error bar for biotinylated goat anti-GFP is clipped at the axis limit (2.5 nM).

extremely slow dissociation rates. We performed a cross comparison of a selection of polyclonal anti-GFP antibodies (chicken and biotinylated goat) as well as a mouse monoclonal anti-6His antibody (N-terminal tag of *E. coli* BirA-GFP).

The BioRad iTaq Universal SYBR green supermix was selected to bring the background Cq value ≥40 at a device concentration of 1 nM and steepen the slope of Cq as a function of antibody concentration. This qPCR mix reduced the PCR efficiency to 1.376 and is better suited to distinguish small changes in *bioO* concentration. All antibodies were coated at a concentration of 2 μg ml^{-1}. The wells were probed with the *E. coli* BirA-GFP : *bioO* device at 2.500, 1.250, 0.625, 0.313 and 0.156 nM (Fig. 5).

The anti-6His antibody bound significantly less *E. coli* BirA-GFP : *bioO* than the polyclonal anti-GFP antibodies. Interestingly, while the chicken anti-GFP captured more *E. coli* BirA-GFP : *bioO* at lower concentrations and plateaued early, the biotinylated goat anti-GFP increased steadily binding the highest number of detection device. Here, we demonstrate that the *E. coli* BirA-GFP : *bioO* can be applied to compare different antibodies and the relative binding capacity of a surface. Our *bioO* and primer combination design and qPCR mix yielding a lower PCR efficiency enables reproducible and more precise determination of intermediate protein concentrations. However, this comes at a cost of reducing the dynamic range and sensitivity of the *E. coli* BirA-GFP : *bioO* detection device.

Conclusions and perspective

Despite its relatively small size, *E. coli* BirA is an exceptionally well-behaved protein offering a variety of functionalities, binding, and catalytic activities. The increased thermostability of *E. coli* BirA-GFP in the presence of ATP, biotin, $MgCl_2$, and *bioO* offers benefits such as extended binding steps and storage at room temperature. There is no doubt that this high-profile protein will be given a special place in the protein chemist's toolbox with its new use as an on–off protein : DNA connection switch. Here, we validated the first application of *E. coli* BirA as a connector between a GFP and a DNA template in various qIPCR assay formats with excellent picomolar detection performance. Our proof-of-concept data should spark the development of further qIPCR-based applications for the detection of protein : protein or protein : ligand interactions. Protein and DNA display technologies requiring reversible high-density DNA or protein arrays, especially in concert with non-dissociating physisorbed or chemisorbed high-affinity IgG, could benefit from the *E. coli* BirA on–off protein : DNA connection switch. We also envisage that droplet digital PCR could be used as an alternative absolute quantitative readout method.[54]

In the last two decades, the flexibility, streamlining and multiplexing power of qPCR for both DNA and protein quantification have created opportunities for the development of innovative bioassays. If combined with other systems such as the Tus : *Ter-lock*,[6] the unique specificity of *E. coli* BirA : *bioO* could offer an avenue for multiplexing or polyplexing qIPCR assays. Interestingly, despite the significantly weaker complex stability[30] and faster dissociation kinetics[21] of *E. coli* BirA : *bioO* compared to Tus : *Ter-lock*,[6,55] both qIPCR technologies perform similarly. Our data suggest that the *E. coli* BirA : *bioO* complex is stable in our qIPCR conditions and that the *bioO* DNA release system is efficient. At a very low antibody concentration, dimerization of the *E. coli* BirA-GFP on *bioO* could be advantageous. Indeed, based on the crystal structure of the holoenzyme dimer,[26] it can reasonably be argued that the two paratopes of an anti-GFP antibody could simultaneously bind to the two GFP in the *E. coli* BirA-GFP : *bioO* detection device, resulting in improved analytical sensitivity due to increased avidity and slower dissociation of the protein complex. This could be particularly valuable for ultrahigh affinity antibody profiling.

E. coli BirA-GFP can be expressed in much higher yields and soluble form than Tus-GFP.[6,42] Other examples of *E. coli* BirA fusion proteins such as CBD-BirA-His have been produced in high yields for protein biotinylation,[44] further supporting the flexibility of *E. coli* BirA for functional fusion protein production. Finally, multiple strategies are available to produce bispecific antibodies[56] offering opportunities to couple a diagnostic antibody with an anti-GFP antibody for ultrasensitive detection with *E. coli* BirA-GFP : *bioO*. In fact, GFP-tagged nanobodies[32] and several combinations of bispecific antibodies with affinity towards GFP or comprising a GFP have already been engineered[33–37] that could easily be implemented in the qIPCR assay formats presented in this work.

Data availability

Data supporting this article have been included as part of the ESI.† Raw data are available upon request from the authors.

Conflicts of interest

There are no conflicts to declare.

Notes and references

1 J. B. Trads, T. Torring and K. V. Gothelf, *Acc. Chem. Res.*, 2017, **50**, 1367–1374.
2 S. Fredriksson, M. Gullberg, J. Jarvius, C. Olsson, K. Pietras, S. M. Gustafsdottir, A. Ostman and U. Landegren, *Nat. Biotechnol.*, 2002, **20**, 473–477.
3 L. Chang, J. Li and L. Wang, *Anal. Chim. Acta*, 2016, **910**, 12–24.
4 S. P. Askin and P. M. Schaeffer, *Analyst*, 2012, **137**, 5193–5196.
5 D. B. Dahdah, I. Morin, M. J. Moreau, N. E. Dixon and P. M. Schaeffer, *Chem. Commun.*, 2009, 3050–3052.
6 I. Morin, N. E. Dixon and P. M. Schaeffer, *Mol. BioSyst.*, 2010, **6**, 1173–1175.
7 I. Morin, S. P. Askin and P. M. Schaeffer, *Analyst*, 2011, **136**, 4815–4821.
8 T. Sano, C. L. Smith and C. R. Cantor, *Science*, 1992, **258**, 120–122.
9 N. R. Pendini, M. Y. Yap, S. W. Polyak, N. P. Cowieson, A. Abell, G. W. Booker, J. C. Wallace, J. A. Wilce and M. C. Wilce, *Protein Sci.*, 2013, **22**, 762–773.
10 B. P. Duckworth, K. M. Nelson and C. C. Aldrich, *Curr. Top. Med. Chem.*, 2012, **12**, 766–796.
11 T. P. Soares da Costa, W. Tieu, M. Y. Yap, N. R. Pendini, S. W. Polyak, D. Sejer Pedersen, R. Morona, J. D. Turnidge, J. C. Wallace, M. C. Wilce, G. W. Booker and A. D. Abell, *J. Biol. Chem.*, 2012, **287**, 17823–17832.
12 O. Prakash and M. A. Eisenberg, *Proc. Natl. Acad. Sci. U. S. A.*, 1979, **76**, 5592–5595.
13 Y. Xu and D. Beckett, *Biochemistry*, 1994, **33**, 7354–7360.
14 Y. Xu, C. R. Johnson and D. Beckett, *Biochemistry*, 1996, **35**, 5509–5517.
15 D. Beckett, E. Kovaleva and P. J. Schatz, *Protein Sci.*, 1999, **8**, 921–929.
16 M. Fairhead and M. Howarth, *Methods Mol. Biol.*, 2015, **1266**, 171–184.
17 M. G. Cull and P. J. Schatz, *Methods Enzymol.*, 2000, **326**, 430–440.
18 A. E. Sorenson, S. P. Askin and P. M. Schaeffer, *Anal. Methods*, 2015, **7**, 2087–2092.
19 S. P. Askin, T. E. H. Bond and P. M. Schaeffer, *Anal. Methods*, 2016, **8**, 418–424.
20 P. R. Adikaram and D. Beckett, *J. Mol. Biol.*, 2012, **419**, 223–233.
21 E. D. Streaker and D. Beckett, *J. Mol. Biol.*, 2003, **325**, 937–948.
22 E. D. Streaker and D. Beckett, *Protein Sci.*, 2006, **15**, 1928–1935.
23 E. D. Streaker and D. Beckett, *Biochemistry*, 2006, **45**, 6417–6425.
24 L. H. Weaver, K. Kwon, D. Beckett and B. W. Matthews, *Protein Sci.*, 2001, **10**, 2618–2622.
25 L. H. Weaver, K. Kwon, D. Beckett and B. W. Matthews, *Proc. Natl. Acad. Sci. U. S. A.*, 2001, **98**, 6045–6050.
26 Z. A. Wood, L. H. Weaver, P. H. Brown, D. Beckett and B. W. Matthews, *J. Mol. Biol.*, 2006, **357**, 509–523.
27 H. Zhao and D. Beckett, *J. Mol. Biol.*, 2008, **380**, 223–236.
28 J. Abbott and D. Beckett, *Biochemistry*, 1993, **32**, 9649–9656.
29 E. D. Streaker and D. Beckett, *Biochemistry*, 1998, **37**, 3210–3219.
30 E. D. Streaker, A. Gupta and D. Beckett, *Biochemistry*, 2002, **41**, 14263–14271.
31 R. Y. Tsien, *Annu. Rev. Biochem.*, 1998, **67**, 509–544.
32 F. Jin, C. Shen, Y. Wang, M. Q. Wang, M. X. Sun and M. Hattori, *Commun. Biol.*, 2021, **4**, 366.
33 K. Tawa, M. Umetsu, T. Hattori and I. Kumagai, *Anal. Chem.*, 2011, **83**, 5944–5948.
34 S. Stamova, A. Feldmann, M. Cartellieri, C. Arndt, S. Koristka, F. Apel, R. Wehner, M. Schmitz, M. Bornhauser, M. von Bonin, G. Ehninger, H. Bartsch and M. Bachmann, *Anal. Biochem.*, 2012, **423**, 261–268.
35 B. Jedlitzke, Z. Yilmaz, W. Dorner and H. D. Mootz, *Angew. Chem., Int. Ed.*, 2020, **59**, 1506–1510.
36 S. Hemmi, R. Asano, K. Kimura, M. Umetsu, T. Nakanishi, I. Kumagai and K. Makabe, *Biochem. Biophys. Res. Commun.*, 2020, **523**, 72–77.
37 A. Alvarez-Cienfuegos, N. Nunez-Prado, M. Compte, A. M. Cuesta, A. Blanco-Toribio, S. L. Harwood, M. Villate, N. Merino, J. Bonet, R. Navarro, C. Munoz-Briones, K. M. Sorensen, K. Molgaard, B. Oliva, L. Sanz, F. J. Blanco and L. Alvarez-Vallina, *Sci. Rep.*, 2016, **6**, 28643.
38 A. E. Sorenson and P. M. Schaeffer, *Methods Mol. Biol.*, 2020, **2089**, 159–166.
39 T. E. H. Bond, A. E. Sorenson and P. M. Schaeffer, *Microbiol. Res.*, 2017, **205**, 35–39.
40 T. E. H. Bond, A. E. Sorenson and P. M. Schaeffer, *Microbiol. Res.*, 2017, **199**, 40–48.
41 M. J. J. Moreau, I. Morin, S. P. Askin, A. Cooper, N. J. Moreland, S. G. Vasudevan and P. M. Schaeffer, *RSC Adv.*, 2012, **2**, 11892–11900.
42 M. J. Moreau and P. M. Schaeffer, *Mol. BioSyst.*, 2013, **9**, 3146–3154.
43 J. M. Ruijter, C. Ramakers, W. M. Hoogaars, Y. Karlen, O. Bakker, M. J. van den Hoff and A. F. Moorman, *Nucleic Acids Res.*, 2009, **37**, e45.
44 S. C. Wu, J. C. Yeung, P. M. Hwang and S. L. Wong, *Protein Expression Purif.*, 2002, **24**, 357–365.
45 H. Zhao, S. Naganathan and D. Beckett, *J. Mol. Biol.*, 2009, **389**, 336–348.
46 H. Zhao, E. Streaker, W. Pan and D. Beckett, *Biochemistry*, 2007, **46**, 13667–13676.
47 A. E. Sorenson and P. M. Schaeffer, *Methods Mol. Biol.*, 2020, **2089**, 69–85.
48 S. Askin, T. E. H. Bond, A. E. Sorenson, M. J. J. Moreau, H. Antony, R. A. Davis and P. M. Schaeffer, *Chem. Commun.*, 2018, **54**, 1738–1741.
49 C. He, G. Custer, J. Wang, S. Matysiak and D. Beckett, *Biochemistry*, 2018, **57**, 1119–1129.

50 S. Song, L. Yang, W. L. Trepicchio and T. Wyant, *J. Immunol. Res.*, 2016, **2016**, 3072586.
51 N. Nath, R. Flemming, B. Godat and M. Urh, *J. Immunol. Methods*, 2017, **450**, 17–26.
52 M. Spengler, M. Adler, A. Jonas and C. M. Niemeyer, *Biochem. Biophys. Res. Commun.*, 2009, **387**, 278–282.
53 D. Jani, E. Savino and J. Goyal, *Bioanalysis*, 2015, **7**, 285–294.
54 H. Schroder, M. Grosche, M. Adler, M. Spengler and C. M. Niemeyer, *Biochem. Biophys. Res. Commun.*, 2017, **488**, 311–315.
55 M. J. Moreau and P. M. Schaeffer, *Mol. BioSyst.*, 2012, **8**, 2783–2791.
56 U. Brinkmann and R. E. Kontermann, *mAbs*, 2017, **9**, 182–212.